



Robotic additive manufacturing system: development of suitable range of process parameters for 3D printing of a large-sized object in PLA polymer

Eduardo Costa Pulquerio¹ · Gustavo Franco Barbosa¹ · Sidney Bruce Shiki¹

Received: 20 February 2024 / Accepted: 27 May 2024

© The Author(s), under exclusive licence to Springer Nature Switzerland AG 2024

Abstract

Additive manufacturing (AM) is a disruptive technology with huge potential to replace traditional manufacturing methods. There is an optimistic perspective to increase the use of AM because several applications were developed, and many ongoing projects are active. AM extrusion technology that uses prefabricated filaments is known as FFF (Fused Filament Fabrication). By coupling a screw extruder to the printing system, the materials are fed simultaneously with the printing, so the technique is known as FGF (Fused Granular Fabrication). Both techniques have slow printing speed that limits their use for mass production. To overcome this disadvantage, a single-screw extruder was coupled to an anthropomorphic robotic arm, configuring the Robotic Additive Manufacturing, suitable for complex and large-sized 3D objects cases. The most important process parameters were set by a suitable experimental campaign, ensuring a regular geometry of the deposited layer. One-layer 200 mm long deposited tracks samples was obtained by the combination of process parameters. After the dimensional measurement, a regression analysis was performed to describe the relationship between the process parameters and the geometry of the layer. The obtained mathematical models were used to set up suitable combination of process parameters for slicing and printing a 3D large-sized object in PLA polymer.

Keywords Robotic additive manufacturing · 3D printing · Extrusion · PLA · Polymer

1 Introduction

Additive manufacturing (AM), also popularly known as 3D printing, is a disruptive manufacturing technology with immense potential to replace traditional manufacturing methods. That potential can provide different courses in areas, such as supply chain, product development, and aggregate services, in product offering [1]. AM has gained great popularity in the media and among researchers from different fields [2].

ASTM recently adopted the nomenclature ‘additive manufacturing’ to replace the previous term ‘Rapid Prototyping’ (RP), which was quite common in industries. The term RP was largely used in the context of product development to

describe technologies that create models and physical prototypes, based on digital modeling [3], i.e., prototypes for evaluating the esthetic, the geometry and the functionality of parts or components before significant financial investments in definitive tools for final manufacture and then for commercialization of the product [4]. AM has assumed an important function in the industrial manufacturing area. It is in use for prototyping, for manufacturing of molds [5] for casting processes [6] and for manufacturing of parts in technological applications [5]. AM allows the customization of a wide spectrum of applications in the automotive industry, aerospace, engineering, biological systems, and food supply chains [2], components for medical surgeries [7], components for medical diagnosis [8], and electronic components [9].

AM provides technological advances for the industry, which allows design freedom in parts and products [5]. Companies have adopted the concept of additive manufacturing or, at least, have already started projects to use it. It is a way to face new challenges in the manufacture of new products or prototypes. Hence, there is an optimistic

✉ Eduardo Costa Pulquerio
eduardopulquerio@gmail.com

¹ Mechanical Engineering Department, Federal University of Sao Carlos, Washington Luís Road, km 235, São Carlos, Sao Paulo 13565-905, Brazil

perspective for future growth in the use of this technology [6]. It has advantages over other manufacturing technologies due to easily creating, modifying, and sharing to manufacture in various locations, according to the convenience of the own company [10].

ASTM F2792-12a standard defines AM as a process of joining materials to obtain objects from a digital 3D model, usually from layer deposition (layer addition), unlike the subtractive manufacturing, whose principle is to obtain an object from the removal of unwanted material from a block of raw material [11]. AM has different technologies in which the printed part acquires the desired geometry and properties in a single or multiple process. In the second case, i.e., multi-step AM, the properties consolidate in the later secondary process [12].

AM based on polymer extrusion are systems with lower cost and huge flexibility of use. Thus, these are factors that contribute to the increase of its use and popularity, even among the non-specialized community [2]. As disadvantages, the parts printed by this method have a very rough finish and have structural defects, for example, porosities and voids [13] that can compromise the properties of the part [14].

The raw material for extrusion-based AM technology is a prefabricated polymeric filaments or polymers in granulated or powdered form. When using prefabricated filaments, the process is known as FFF—Fused Filament Fabrication—[15]. On the other hand, in case of feeding granulated or powdered polymers directly into the extruder feed system [16], the process is known as FGF—Fused Granular Fabrication—[17] or FPF—Fused Particle Fabrication—[18]. Due to the use of an extruder coupled to the printing system, the FGF technology has advantages over the FFF because FGF allows the manufacturing of printed components using a broader range of materials, such as polymeric blends, polymeric matrix composites [17], and recycled polymers [19], such as polypropylene that is massively in consumer products [20]. The FGF AM technology has an industrial screw extruder coupled to manipulator that enables the use of polymer blends or composites to meet specific properties or characteristics for parts in technological applications. About composites, one of the candidates for application that requires high mechanical strength is the carbon fiber reinforced polymers (CFRP) [21].

Despite of the benefits of the extrusion-based AM, the FFF and FGF processes have limitations in terms of printing speed since the observed low mass deposition speeds limit their use for large-scale production. In this context, the use of an industrial extruder coupled to an anthropomorphic robot emerges as a solution as it allows a material deposition rate in order of 10 to 20 times higher than in commercial FFF systems [22]. Hence, a series of advantages appear, such as productivity gains; obtaining larger

quantities of printed pieces; possibility of improving the repeatability of the manufacturing process [23]; improvement in the dimensional tolerance of the part [24]. The use of anthropomorphic robots with long reach coupled to the printing systems enables the modeling of long-sized parts with reduction or elimination of their partitioning, which is a factor pointed out as a goal and target for future work in modern polymer extrusion AM systems [25] becoming future challenges in terms of processing and materials. From the processing perspective, increasing the size of the part provides critical challenges due to the longer time required for manufacturing, the greater probability of warping [26] and the formation internal voids [27] in the part. According to Wang et al. (2016), it is necessary to optimize the extrusion process to minimize those critical potential problems. The author proposed extrusion with variable pitch and screw geometry with progressive diameter. In addition, Li et al. (2002) propose geometry formats for the extrusion die section to control the shape of the extruded material, thus minimizing the density of internal voids in the printed parts. Another problem when printing large-sized parts is related to the difficulty to react dimensional accuracy after successively deposited layers [28]. The author proposed a real-time correction of the piece slicing (re-slicing) for more accurate dimensional control. Regarding the materials perspective, it is necessary to develop AM using structural materials because pure polymers have limited mechanical strength for functional printed parts, which imposes difficulties for technological application in different industries [24]. Hence, to overcome the materials challenge, it is possible to use polymeric matrix composites with reinforcements (particles, fiber, including nanomaterials) [29], so achieving a better balance of mechanical, electrical, and thermal properties [24]. Using the finite Element analysis (FEA or FEM) method, there is the possibility of predictability of the behavior of 3D printed structures polymers [30] which allow the possibility of improving the combination of materials and geometry of the part. The extrusion-based AM-FGF technology allows the development of those advanced blends and composites materials with driven-properties to specific engineering requirements [31]. AM with structural polymeric matrix composites is object in studies to replace metallic parts in market segments, such as aeronautics and automobile [32], and naval [33].

In summary, the manufacturing of parts: quicker; with better process repeatability; the large-sized pieces; with higher mechanical strength; with better dimensional accuracy are the main challenges for the future of polymer extrusion AM technology.

The objective of this experimental campaign is to synchronize the main parameters of the printing process, verifying the effect of them on the geometry of the printed layer. The main parameters of the printing process have been set

to guarantee the regularity of the deposited layer. The samples format were single-layer rectilinear tracks (deposited on a printing trajectory). The parameters under study are: 1) Extruder screw rotation speed (w_m); 2) Robot translation speed (v_t); and 3) Nominal layer height (Δz_{ref}).

It was possible to obtain samples combining variations of w_m (20, 30 and 40 rpm), v_t (15, 20 and 25 mm/s) and Δz_{ref} (1.50, 2.00, 2.50 mm), then it was possible to measure the average height ($h_{z_{mean}}$) and average width ($w_{dt_{mean}}$) of the tracks. The subtraction of Δz_{ref} by $h_{z_{mean}}$ determined the difference between nominal and measured mean layer height (Δz_{diff}). Mathematical regression analysis has been performed to describe the correlation between the process parameters versus $w_{dt_{mean}}$, versus Δz_{diff} , and versus $h_{z_{mean}}$. Hence, generating regression models for combinations of process parameters to predict the adequate flow of polymer that provide a null (or close to null) difference in Δz_{diff} , and to estimate the height and the width values for the deposited layer. Those values were used as input data for the slicing software to manufacture a selected larger 3D part.

2 Materials and methods

2.1 Materials

2.1.1 Raw material

The raw material used in the experiment is PLA (polylactic acid) polymer, brand Ingeo Biopolymers, grade 4043D, manufactured by NatureWorks. PLA is widely used in extrusion-based additive manufacturing, even when in filament form, due to its good processability. So for starting trials using the robotic additive manufacturing system, PLA polymer was chosen to generate a knowledge base for future experiments.

2.1.2 Equipment

This experimental campaign explores additive manufacturing technology via fused granular fabrication with robotic process automation. The equipment used is a Robotic Additive Manufacturing System composed by an industrial single-screw extruder coupled to an anthropomorphic robotic arm (robot with six axes, 88 kg payload, and 2,236 mm of horizontal reach). The extruder derives from the “micro extruders” product family, and it has a pellet feeding system (hopper), three heated zones and a conic deposition nozzle (with a \varnothing 1.75 mm hole).

Beyond the single-screw extruder and the robotic arm, the 3D printing system has also a feedstock device (for raw material in powder or pellet form) and a large-sized heated print bed (1000 × 1000 mm).

That equipment was designed and developed at the Additive Manufacturing and Automation Research Center (AMARC) of the Department of Mechanical Engineering at the Federal University of São Carlos (DEMec/UFSCar), in Brazil. The robotic additive manufacturing system is presented in Fig. 1.

2.2 Methods and experimental design

The steps adopted as methodology in this experimental work are illustrated in Fig. 2.

The process parameters for the polymer extrusion are constant (Table 1). Those parameters refer to the dehumidification of the polymer, the temperature of the heating zones of the extruder, and the temperature of the print bed. Extrusion processing was set up based on typical recommendation of the PLA manufacturers. The suggested process parameters are: temperature range from 180 to 200 °C, screw speed from 20 to 100 rpm and dehumidification during 4 h at 80 °C.

The main process parameters have been adjusted to guarantee the regularity of the deposited layer. The parameters are extruder screw rotation speed (w_m), robot translation speed (v_t), and nominal layer height (Δz_{ref}). An experimental design combining variations of w_m (20, 30, and 40 rpm), v_t (15, 20, and 25 mm/s) and Δz_{ref} (1.50, 2.00, and 2.50 mm) were obtained (Table 3). The combinations of test possibilities are $3 \times 3 \times 3 = 27$ different experimental conditions. When repeated three times, they totaled eighty-one samples. Every sample is a 200 mm long single-layer rectilinear track, which can be interpreted as a single layer deposited on a printing path.

The extrusion of molten polymers normally promotes a significant amount of extensional flow [35], which impacts the final properties of polymeric feedstock products. Divergent flow is also observed with the expansion of the flow front, into the radial direction, of the extruded polymer at the exit of the extrusion die as a bioriented extensional flow [35]. This paper deals with the development and synchronization of printing process parameters. It can be noticed that the combination between the robot translation speed and the extruder screw rotation speed can increase or decrease the expansion of the divergent flow, in the radial direction, and the extensional flow, at the exit of the extruder die. This means influence on the final diameters of the deposited layer in the printing process. Thus, Δz_{ref} equal to 2.0 mm has been established as an initial reference for process development in the printing system used. After cooling, the samples height (h_z) and the width (w_{dt}) have been measured using a Mitutoyo Digimatic CD-8" ASX caliper (with a resolution of 0.01 mm). The measurements were in five regions of the sample, equally spaced, generating the average of the values, $h_{z_{mean}}$ and $w_{dt_{mean}}$, respectively. The difference between the

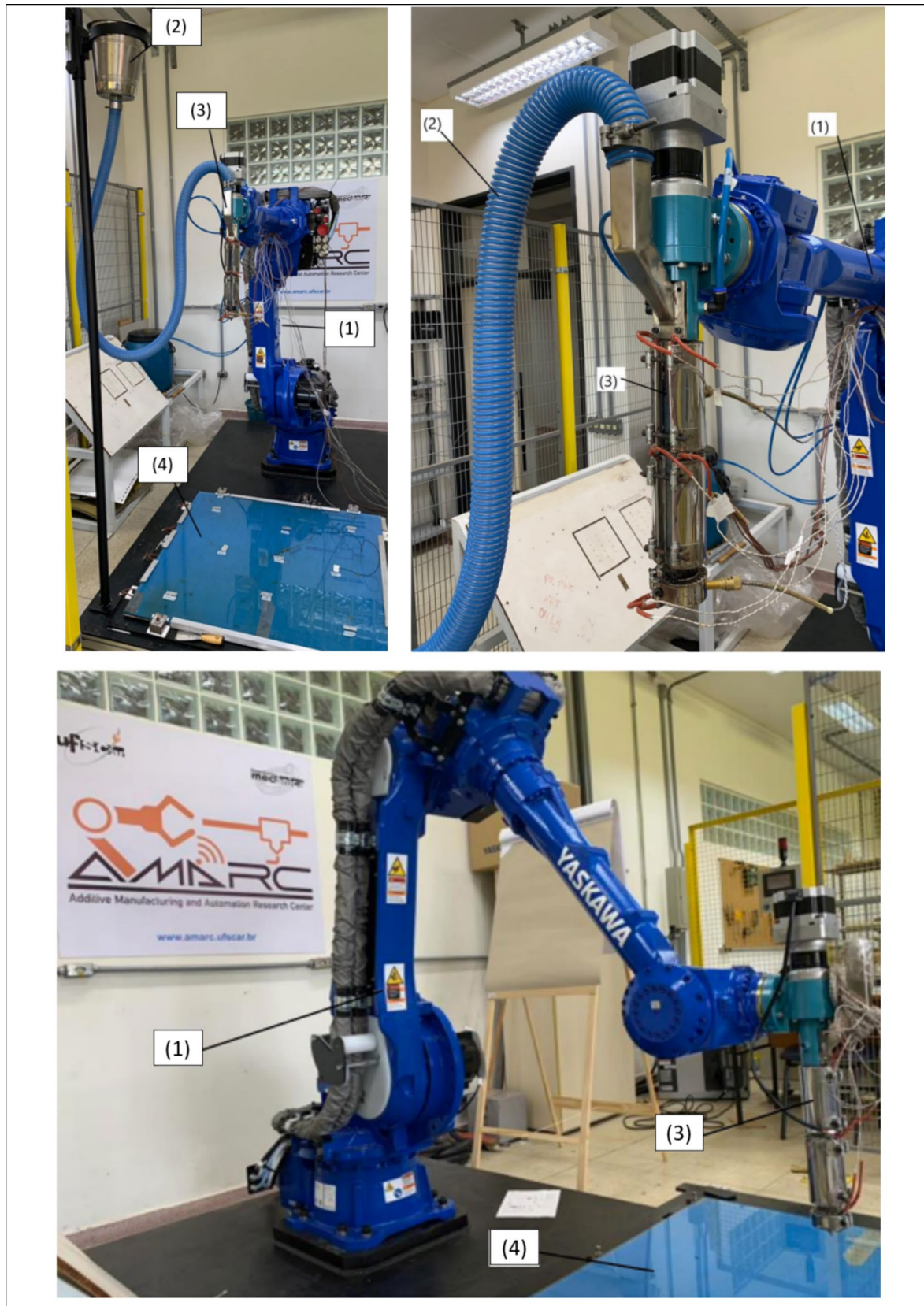


Fig. 1 Robotic Additive Manufacturing System. 1 Anthropomorphic robotic arm, 2 feedstock device, 3 Single-screw extruder, 4 Heated print bed. Source: [34]

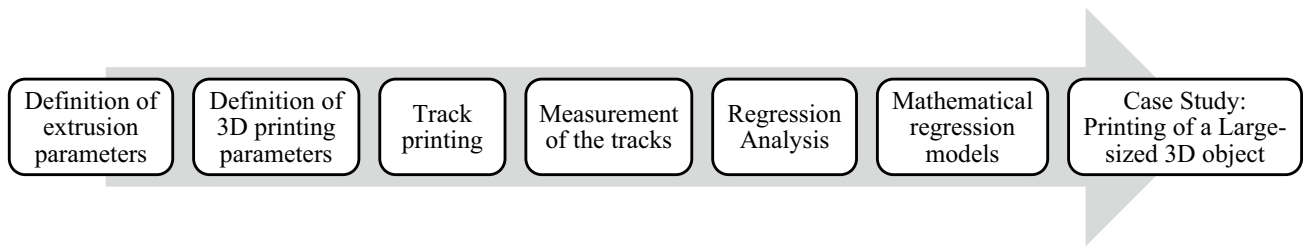


Fig. 2 Flowchart of the steps of the experiment methodology

Table 1 Process parameters for the polymer extrusion

Factor	Value	Unit
Dehumidification–Temperature	80	°C
Dehumidification–Time	4	H
Extruder–Temperature Zone 1 (T ₁)	175	°C
Extruder–Temperature Zone 2 (T ₂)	180	°C
Extruder–Temperature Zone 3/Nozzle (T ₃)	190	°C
Print Bed–Temperature (T _{hb})	RT ^a	°C

^aRT Room Temperature

nominal fillet height (Δz_{ref}) and the average height (hz_{mean}) was calculated by the Eq. 1.

$$\Delta z_{diff} = \Delta z_{ref} - hz_{mean} \tag{1}$$

Track uniformity was analyzed through the ratio between the average height (hz_{mean}) and average width (wdt_{mean}), calculated by the Eq. 2.

$$U = \frac{hz_{mean}}{wdt_{mean}} \times 100 \tag{2}$$

After obtaining data correlating the process parameters ($w_m, v_t, e \Delta z_{ref}$) versus Δz_{diff} , versus hz_{mean} , and versus wdt_{mean} , a regression analysis was performed to describe the interaction between the variables through a mathematical regression model. Because the process parameters ($w_m, v_t, e \Delta z_{ref}$) simultaneously impacts the response in Δz_{diff} , hz_{mean} , and wdt_{mean} , a multiple regression analysis was adopted. The layer geometry values calculated by the mathematical models were used as input data for slicing and then manufacturing a selected large-sized 3D part.

Table 2 Experimental design for the printing process parameters and samples

Factor	Symbol	Unit	Value
Extruder screw rotation speed	w_m	rpm	20/25/30
Robot translation speed	v_t	mm/s	15/20/25
Nominal layer height	Δz_{ref}	mm	2
Track sample length	–	mm	200
Quantity of layers	–	un	1

3 Results and discussion

3.1 Uniformity of the deposited layer and stability of the extrusion process

Using the process parameters for polymer extrusion (Table 1) and applying the combinations of parameters for the printing process (Table 2), samples were obtained in the form of 200 mm long single-layer rectilinear track, in a single layer deposited on a printing path. An example of sample can be found on Fig. 3.

The Robotic Additive Manufacturing system used could produce extruded polymer flow without interruption in all tests, which demonstrates that the polymer transformation process parameters (Table 1), together with the screw rotation parameter— w_m —(Table 2) generated sufficient shear rate to melt the PLA polymer and so generate continuous extrusion. After cooling, the samples height (hz) and the width (wdt) were measured using a Mitutoyo Digimatic CD-8" ASX caliper (with a resolution of 0.01 mm). The measurements were taken in five regions of the sample, equally spaced, generating the average of the values, hz_{mean} and wdt_{mean} , respectively. The difference between the nominal fillet height (Δz_{ref}) and the average height (hz_{mean}) was calculated by the Eq. 1, resulting in Δz_{diff} . The track uniformity (U) was calculated by Eq. 2. The uniformity of the deposited layer was evaluated through the ratio between h_{mean} and wdt_{mean} (Eq. 3). The results are presented on Fig. 4.

The smaller the difference between the magnitude height and width, in the same experimental condition, the more

Fig. 3 Single-layer rectilinear track used as sample on this experimental work. **a** Representation of the layer deposition process; **b** Example of the obtained tracks

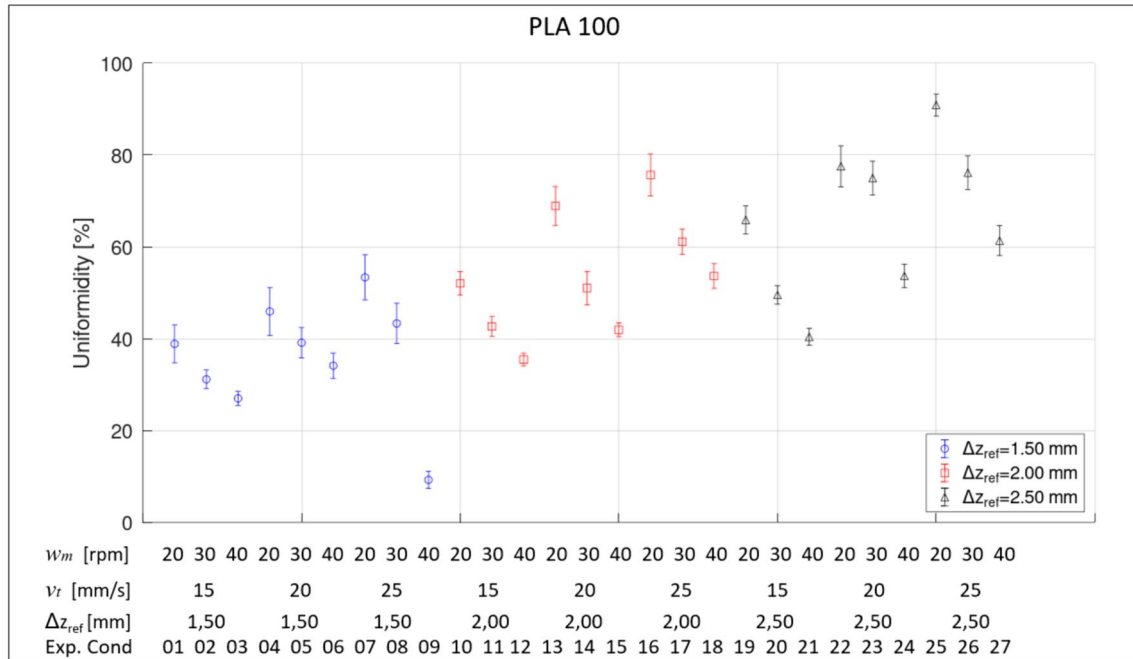
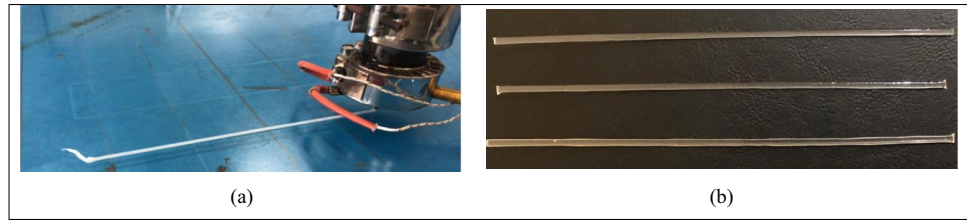


Fig. 4 Uniformity of the deposited layers for PLA Polymer

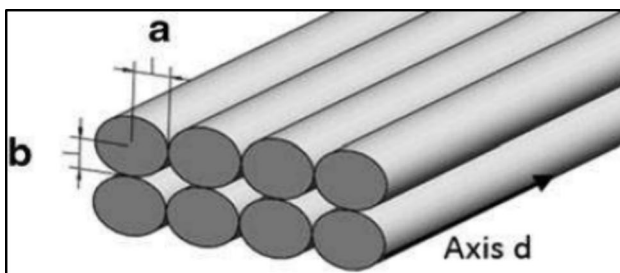


Fig. 5 Ideal cross section that minimizes the density of voids in the manufacture of printed parts according to the model proposed by Li et al. (2002); ‘a’ is half the width and ‘b’ half the height of the deposited filament. Source: [26]

uniform the layer is, so the cross section of the extruded track is more like a circle. The greater the difference between height and width, the cross section of the extruded track resembles an ellipse. Li et al. (2002) proposed a theoretical

model to analyze the effect of void density in the deposited printing layers. The ideal condition to minimize the density of voids during printing is the deposition of an extruded layer with a cross section closer to an ellipse [27], as represented in Fig. 5. According to Magnoni et al. (2017), more uniform extruded layers, with a cross section resembling a circle, i.e., like cylindrical tracks simply deposited on the printing bed, are harmful from the point of view of part manufacturing.

Figure 4 demonstrates that the lower the nominal height (Δz_{ref}), there is a greater tendency for the deposited layer to obtain a cross section more like an elliptical section. The tests conducted with $\Delta z_{ref} = 1.50$ mm showed better results since the cross section of the deposited layers more closely resembled ellipses. The tests conducted with $\Delta z_{ref} = 2.50$ mm had worse results because the cross section of the deposited fillets was more like circles. As extremes, experimental condition 09 ($w_m = 40$ rpm; $v_t = 25$ mm/s;

$\Delta z_{ref}=1.50$ mm), provided the best appearance with tracks with a non-uniform cross-Sect. (9.25%), therefore elliptical, while the experimental condition 25 ($w_m=20$ rpm; $v_t=25$ mm/s; and $\Delta z_{ref}=2.50$ mm) presented the worst appearance with very uniform fillets (90.87%), therefore, cylindrical. Therefore, experimental condition 25 is not satisfactory from a manufacturing point of view, as the cross section resembling circles is an undesirable condition according to the observations of Magnoni et al. (2017).

3.2 The printing process and characteristics of the tracks

Figures 6, 7, 8 present the results of Δz_{diff} , h_{mean} e $w_{dt_{mean}}$, respectively.

The obtained standard deviations of height and width were low, which demonstrated good stability of the printing system. None of the experimental conditions under study presented null Δz_{diff} . Figure 6 demonstrates that in

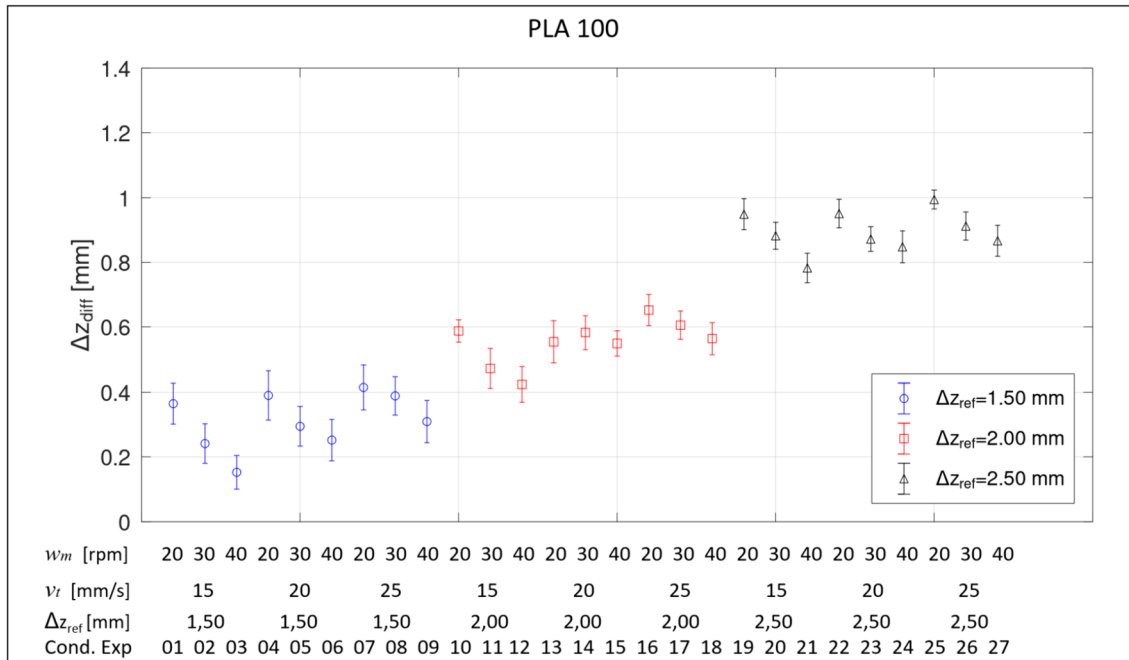


Fig. 6 Individual plot of the difference between nominal and real heights (Δz_{diff}). The circles, squares and triangles represent the average values, and the bars represent the standard deviation

Fig. 7 Individual plot of the average height value ($h_{z_{mean}}$). The circles, squares and triangles represent the average values, and the bars represent the standard deviation

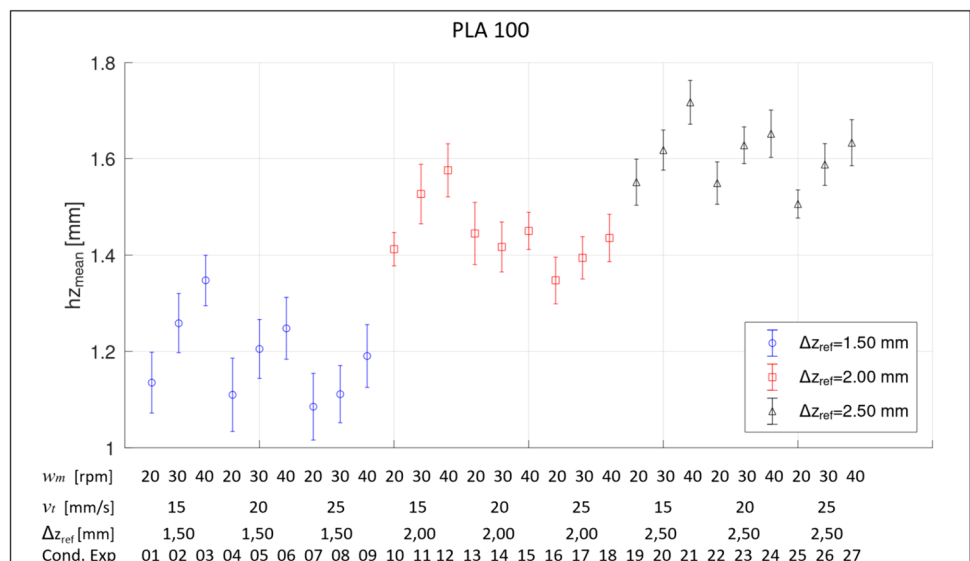
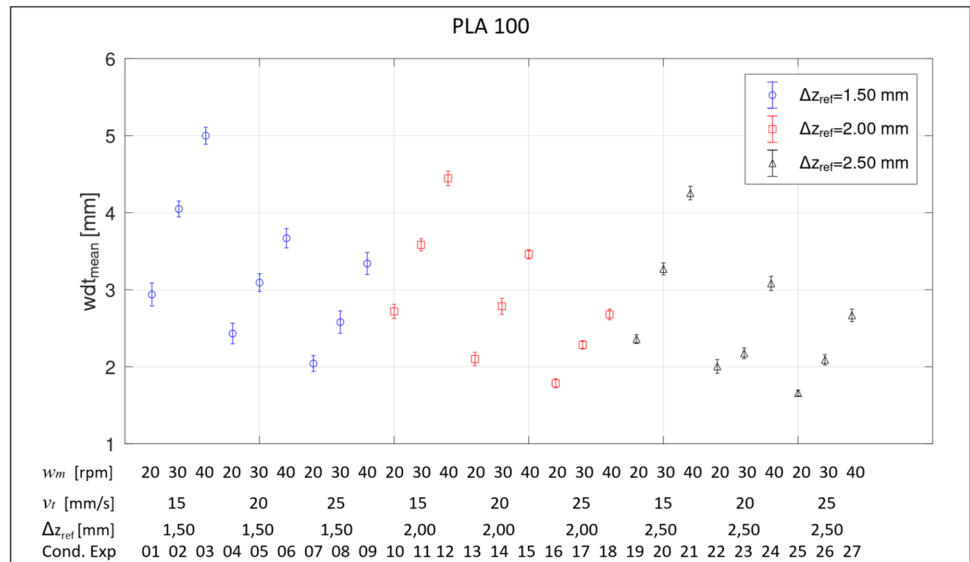


Fig. 8 Individual plot of the average width value (w_{dt_mean}). The circles, squares and triangles represent the average values, and the bars represent the standard deviation



all process combinations evaluated, the average track height (h_{z_mean}) was below the corresponding nominal height (Δz_{ref}). The conditions with the process parameter Δz_{ref} equal to 1.5 mm were those that resulted in Δz_{diff} closer to zero, i.e., with lower experimental error between nominal and real heights. The smallest height errors found occur in process conditions 01 to 09 (Δz_{ref} adjusted to 1.5 mm). The experimental conditions 02 ($w_m = 30$ rpm; $v_t = 15$ mm/s e $\Delta z_{ref} = 1.50$ mm), 03 ($w_m = 40$ rpm; $v_t = 15$ mm/s e $\Delta z_{ref} = 1.50$ mm), and 05 ($w_m = 30$ rpm; $v_t = 20$ mm/s e $\Delta z_{ref} = 1.50$ mm) presented the lowest Δz_{diff} values.

The results suggest that to obtain Δz_{diff} with lower experimental error, it is necessary to combine faster extruder screw rotation (w_m), slower robot translation speed (v_t), and smaller nominal layer height (Δz_{ref}). Reducing v_t would represent a decrease in the productivity of the printing process, opposing the objectives of this work. That was a non-feasible

intervention. To operate with higher w_m , it is necessary to have attention to the thermal stability of the polymer and the torque capacity of the extruder servomotor. In the first case, the rotation limit and the temperature generated in the extrusion process must not cause degradation in the polymer. The motor of the industrial extruder used did not demonstrated enough torque capacity to operate above 40 rpm during PLA processing due to decoupling between the gear motor and the extruder servomotor, which made it impossible to explore data in experimental conditions with higher extruder screw rotations. Thus, the only process variable that would allow exploring null (or closest to null) Δz_{diff} values is Δz_{ref} . Hence, combination of process parameters with Δz_{ref} smaller than 1.5 mm for pure PLA polymer sounds better option for exploration. Close to zero (null) values of Δz_{diff} is desirable from the manufacturing point of view to obtain good dimensional accuracy of the printed parts. In this concept, the tests with Δz_{ref} equal to 1.50 mm were more appropriate.

Figure 7 and 6c demonstrates that, at the same robot translation speed, the increase in extruder rotation represented an increase in the average height and width of the deposited track, due to the greater amount of extruded polymer available for deposition in the printing process. In all tested process combinations, an increase in the average height was noted with the increase in extruder screw

Table 3 PLA Polymer: Results of Multiple variable regression analysis: p-values

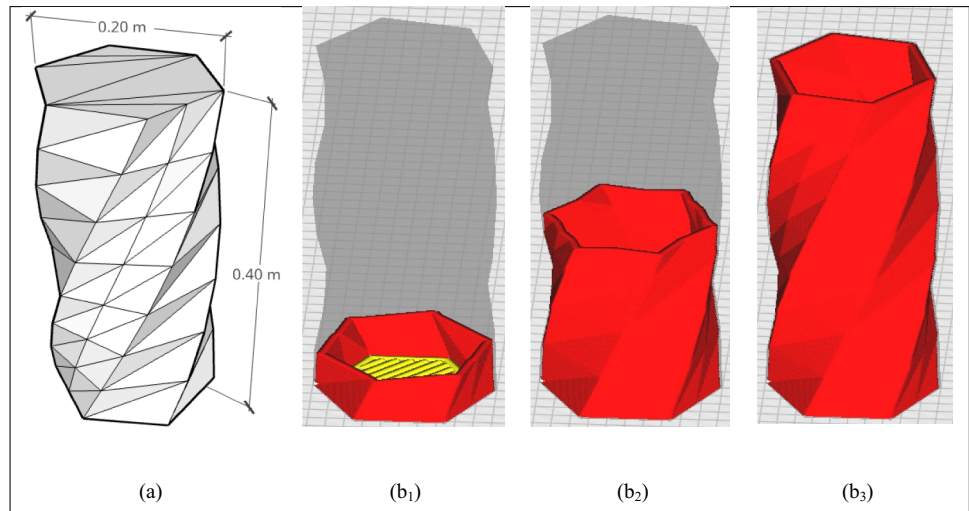
Factor	p-values		
	Δz_{diff}	h_{z_mean}	w_{dt_mean}
Intersection	2.57×10^{-2}	2.57×10^{-2}	6.60×10^{-14}
w_m	8.76×10^{-3}	8.76×10^{-3}	2.17×10^{-10}
v_t	4.24×10^{-1}	4.24×10^{-1}	1.56×10^{-12}
Δz_{ref}	6.07×10^{-15}	2.08×10^{-5}	8.50×10^{-4}
$w_m \cdot v_t$	8.91×10^{-3}	8.91×10^{-3}	1.40×10^{-16}
$w_m \cdot \Delta z_{ref}$	4.73×10^{-1}	4.73×10^{-1}	9.75×10^{-3}
$v_t \cdot \Delta z_{ref}$	2.07×10^{-2}	2.07×10^{-2}	1.94×10^{-2}
w_m^2	5.61×10^{-1}	5.61×10^{-1}	1.00×10^{-1}
v_t^2	8.82×10^{-1}	8.82×10^{-1}	2.45×10^{-12}
Standard deviation [mm]	± 0.04	± 0.04	± 0.12
R^2_{adj} [%]	97.32	95.19	98.12

Table 4 3D Printing process parameters for used slicing strategy

Data for the printing process (imputed in regression mathematical models)			Data for the slicing procedure (output of the regression model then imputed for slicing procedure)		
w_m [rpm]	v_t [mm/s]	Δz_{ref} [mm]	Δz_{diff}^a [mm]	hz [mm]	wdt [mm]
40	15	1.50	0.15 ± 0.06	1.35 ± 0.06	4.95 ± 0.14

^a Δz_{diff} is the height of the first printing layer. From the second layer onwards, the layers heights used are Δz_{ref}

Fig. 9 a 3D Model.STL of a larger-sized part; (b₁, b₂ and b₃) Representation of the material deposition way layer by layer. Source: The authors



rotation. However, it is not possible to state that at rotations even higher than those tested, there would be a balance in the average height according to the nominal height, despite the results obtained suggest this behavior.

Regarding the average width of the tracks (Fig. 6c), it has noted a similar behavior in which increasing the extruder rotation provided an increase of the width of the track. The track width is a consequence of the selected process parameters. In other words, you can define combinations of process parameters that achieve a desired printed layer height, then the width is a consequence. The height and width values are data for the part slicing strategy.

3.3 Regression analysis

Regression analysis with multiple variables has been performed to correlate the relation of the process parameters ω_m , v_t and Δz_{ref} with the results–responses in Δz_{diff} , hz_{mean} and wdt_{mean} of the printed tracks. The results of the analyses demonstrated how the process parameters and how the interactions between the parameters are influenced the responses. The main results of the regression analysis (p-value and estimated standard deviation) are in Table 3, while the estimated regression models for the Δz_{diff} , hz_{mean} and wdt_{mean} responses, expressed by Eqs. 3, 4 and 5, respectively. The adequacy of the regression models is demonstrated by the high coefficients of determination (R^2_{adj}): 97.32%, 95.19%, and 98.12%, respectively.

$$\begin{aligned} \Delta z_{diff} = & (-0,5371) + (-0,0189 \times \omega_m) + (0,0137 \times v_t) \\ & + (0,6833 \times \Delta z_{ref}) + [0,0004 \times (\omega_m \times v_t)] \\ & + [0,0010 \times (\omega_m \times \Delta z_{ref})] + [-0,0065 \times (v_t \times \Delta z_{ref})] \\ & + (0,0001 \times \omega_m^2) + (-0,0001 \times \vartheta_t^2) \end{aligned} \quad (3)$$

$$\begin{aligned} hz_{mean} = & 0,5371 + (0,0189 \times \omega_m) + (-0,0137 \times v_t) \\ & + (0,3167 \times \Delta z_{ref}) + [-0,0004 \times (\omega_m \times v_t)] \\ & + [-0,0010 \times (\omega_m \times \Delta z_{ref})] + [0,0065 \times (v_t \times \Delta z_{ref})] \\ & + (-0,0001 \times \omega_m^2) + (0,0001 \times \vartheta_t^2) \end{aligned} \quad (4)$$

$$\begin{aligned} wdt_{mean} = & 6,1517 + (0,1459 \times \omega_m) + (-0,4085 \times v_t) \\ & + (-0,6814 \times \Delta z_{ref}) + [-0,0041 \times (\omega_m \times v_t)] \\ & + [-0,0103 \times (\omega_m \times \Delta z_{ref})] + [0,0185 \times (v_t \times \Delta z_{ref})] \\ & + (0,0005 \times \omega_m^2) + (0,0092 \times \vartheta_t^2) \end{aligned} \quad (5)$$

The obtained mathematical regression models are useful to select suitable combination of process parameters. Equation 3 calculates combinations of process parameters that guarantee a null (or close to null) height difference (Δz_{diff}), i.e., combinations between the extruder screw rotation speed and the robot translation speed which provide appropriated polymer throughput for the layer height set in the robot motion control. For example, to achieve the highest productivity by elevating the levels of extruder screw rotation speed and robot translation speed, Eq. 3 provides the suitable value of nominal layer height. After setting up the process with Eq. 3, both Eqs. 4 and 5 estimate the track height and width values, respectively, which are useful as input data in slicing software's for manufacturing objects or complex 3D parts.

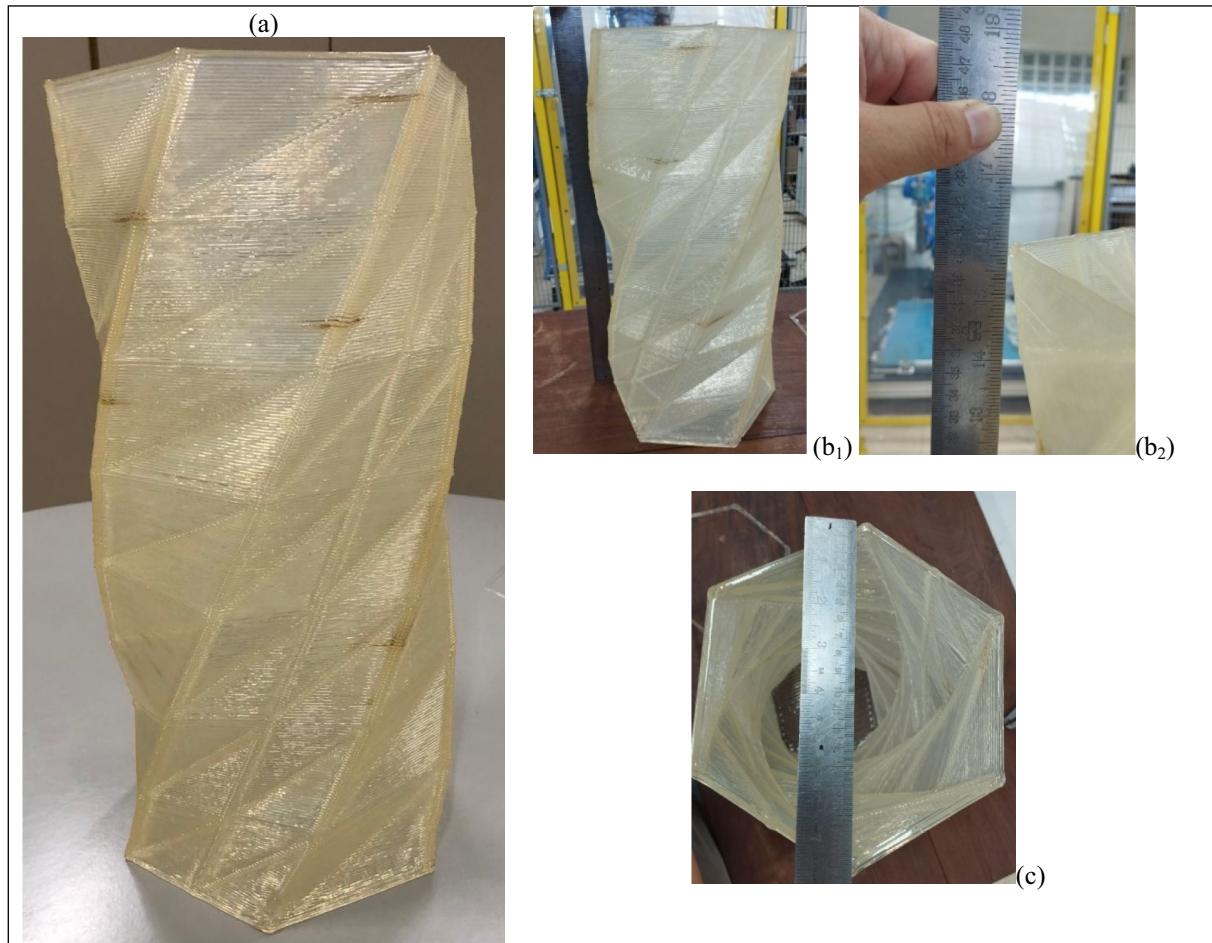


Fig. 10 a Final example of a large-sized object obtained with the described setup: a vase made in PLA polymer, natural color; (b₁ and b₂) demonstration of the vase height; and c demonstration of the vase width. Source: The authors

4 Case study

As a case study, a large-sized piece of home decor & gardening has been realized using the considered setup running with the process parameters found in Sect. 3.3 (Eqs. 3, 4 and 5). The selected parameters are in Table 4. The inputted data for the printing process (Table 4) was chosen to generate null or close to null Δz_{diff} , considering the quicker as possible way to manufacture the part of the case study.

Ultimaker Cura 5.5.0 software, which functions as a CAD/CAM software, generated the printing trajectory, i.e., the motion instructions for the robot (Fig. 7).

The printing system was able to produce the vase (Fig. 8) in about 3.40 h, with a mass of 1402 g in PLA polymer. With that 3D printing strategy, the system had a deposition flow rate of about 333 cm³/h (Fig. 9). The quantity of printed layers is 296 layers. The measured dimensions of the vase in comparison to the nominal dimensions are:

- heightreal 403 ± 1 [mm] vs. nominal 400 mm. Result: +0.65% difference.
- widthreal 198 ± 1 [mm] vs. nominal 200 mm. Result: -1.10% difference.
- wall thickness: real 5.20 ± 0.25 [mm] vs. nominal 4.95 mm. Result: +5.05% difference.

The case study demonstrated the effectiveness of the approach presented in this paper, which is composed by an experimental campaign designed to find a suitable range of process parameters to guarantee a regular shape of deposited tracks for each layer (Fig. 10).

5 Conclusions

The main objective of this study, to develop an adequate range of process parameters that would guarantee a regular deposition of layers for 3D printing of parts in a robotic additive manufacturing system, was achieved. The combinations

of process parameters generated samples whose geometry was measured and, after multiple regression analysis, generated mathematical models to predict the geometry (height, width) of the layer deposited in the 3D printing process for PLA. The successful in the case study demonstrated the effectiveness of the approach presented in this paper.

The novelty of this proposal aims to present the use of a robot to assist the extrusion-based additive manufacturing. The use of an industrial extruder coupled to an anthropomorphic robot emerges as a solution because it allows quicker material deposition rate than in commercial extrusion-based additive manufacturing systems. Main contribution fits into the development of suitable range of process parameter for 3D printing of pieces, especially for the large-sized ones, using the robotic additive manufacturing system developed by the authors.

During the trials, the motor of the micro-extruder had limited torque capacity. This behavior had impeded to explore a broader range of extruder screw rotation in higher speed. The authors are improving the Robotic Additive Manufacturing System by replacing the motor for a higher torque capacity one to make feasible work with higher viscosity polymers and/or in higher screw rotation.

The main objectives of this work were achieved and, considering the results obtained, it is suggested for future work:

- Explore a range of process combinations that consider extruder screw rotations above 40 rpm and robot transaction speeds above 25 mm/s, with the aim of promoting productivity gains, that is, layer deposition rates even higher than those obtained in this work;
- Expand the use of the proposed methodology to a wider range of materials, such as
 - o Polymers: ABS, PA, PC, PET-g, OS, and TPU;
 - o Polymeric blends: ABS/PC, ABS/PLA and PC/PET-g;
 - o Composite materials, including biocomposites, nanocomposites, and plant fibers reinforcement.
 - o Note: The effectiveness of using the methodology of this work was applied to the ABS polymer in a previous study [36].

Supplementary Information The online version contains supplementary material available at <https://doi.org/10.1007/s40964-024-00685-y>.

Acknowledgements We thank the support from the Federal University of São Carlos (UFSCar). Any opinions, findings, and conclusions or recommendations expressed in this paper are those of the authors and do not necessarily reflect the views of the Federal University of São Carlos.

Funding This work was supported by Sao Paulo Research Foundation (FAPESP) for Grant #2019/22115-0, and the National Council for

Scientific and Technological Development (CNPq) for his technological productivity fellowship (Process #302814/2021-3).

Data availability The data will be available based on the demand of the readers.

Declarations

Conflict of interest On behalf of all authors, the corresponding author states that there is no conflict of interest.

References

1. Jiang R, Kleer R, Piller FT (2017) Predicting the future of additive manufacturing: a Delphi study on economic and societal implications of 3D printing for 2030. *Technol Forecast Soc Change* 117:84–97. <https://doi.org/10.1016/j.techfore.2017.01.006>
2. Gao W, Zhang Y, Ramanujan D et al (2015) The status, challenges, and future of additive manufacturing in engineering. *Comput Aided Des* 69:65–89. <https://doi.org/10.1016/j.cad.2015.04.001>
3. Gibson I, Rosen D, Stucker B (2015) *Development of Additive Manufacturing Technology*. Additive Manufacturing Technologies. Springer, New York, New York, NY, pp 19–42
4. Pham DT, Gault RS (1998) A comparison of rapid prototyping technologies. *Int J Mach Tools Manuf* 38:1257–1287. [https://doi.org/10.1016/S0890-6955\(97\)00137-5](https://doi.org/10.1016/S0890-6955(97)00137-5)
5. Thompson MK, Moroni G, Vaneker T et al (2016) Design for additive manufacturing: trends, opportunities, considerations, and constraints. *CIRP Ann* 65:737–760. <https://doi.org/10.1016/j.cirp.2016.05.004>
6. Tang S, Yang L, Fan Z et al (2021) A review of additive manufacturing technology and its application to foundry in China. *China Foundry* 18:249–264. <https://doi.org/10.1007/s41230-021-1003-0>
7. Shi Y, Wu X, Paydarfar JA, Halter RJ (2021) Imaging-compatible oral retractor system for use in image-guided transoral robotic surgery. In: Linte CA, Siewerdsen JH (eds) *Medical Imaging 2021: Image-guided procedures, robotic interventions, and modeling*. SPIE, p 4
8. Alrashoudi AA, Albalawi HI, Aldoukhi AH et al (2021) Fabrication of a lateral flow assay for rapid in-field detection of COVID-19 antibodies using additive manufacturing printing technology. *Int J Bioprint* 7:399. <https://doi.org/10.18063/ijb.v7i4.399>
9. Lanzolla AML, Attivissimo F, Percoco G et al (2022) Additive manufacturing for sensors: piezoresistive strain gauge with temperature compensation. *Appl Sci (Switzerland)*. <https://doi.org/10.3390/app12178607>
10. Hu C, Qin QH (2020) Advances in fused deposition modeling of discontinuous fiber/polymer composites. *Curr Opin Solid State Mater Sci*. <https://doi.org/10.1016/j.cossms.2020.100867>
11. ASTM International (2012) Designation F2792–12a: Standard Terminology for Additive Manufacturing Technologies (Withdrawn 2015). ASTM International, West Conshohocken, PA
12. ASTM International (2021) *Additive Manufacturing, Design, Functionally Graded Additive Manufacturing*. ASTM International, 100 Barr Harbor Drive, PO Box C700, West Conshohocken, PA 19428–2959
13. Pandey PM, Reddy NV, Dhanda SG (2003) Improvement of surface finish by staircase machining in fused deposition modeling. *J Mater Process Technol* 132:323–331. [https://doi.org/10.1016/S0924-0136\(02\)00953-6](https://doi.org/10.1016/S0924-0136(02)00953-6)

14. Agarwala MK, Jamalabad VR, Langrana NA et al (1996) Structural quality of parts processed by fused deposition. *Rapid Prototyp J* 2:4–19. <https://doi.org/10.1108/13552549610732034>
15. Beniak J, Šooš L, Križan P et al (2022) Resistance and strength of conductive PLA processed by FDM additive manufacturing. *Polymers (Basel)*. <https://doi.org/10.3390/polym14040678>
16. Sun C, Wang Y, McMurtrey MD et al (2021) Additive manufacturing for energy: a review. *Appl Energy*. <https://doi.org/10.1016/j.apenergy.2020.116041>
17. Cheng T, Wood D, Kiesewetter L et al (2021) Programming material compliance and actuation: Hybrid additive fabrication of biocomposite structures for large-scale self-shaping. *Bioinspir Biomim*. <https://doi.org/10.1088/1748-3190/ac10af>
18. Woern AL, Pearce JM (2018) 3-D printable polymer pelletizer chopper for fused granular fabrication-based additive manufacturing. *Inventions*. <https://doi.org/10.3390/inventions3040078>
19. Reich MJ, Woern AL, Tanikella NG, Pearce JM (2019) Mechanical properties and applications of recycled polycarbonate particle material extrusion-based additive manufacturing. *Materials*. <https://doi.org/10.3390/ma12101642>
20. Spoerk M, Holzer C, Gonzalez-Gutierrez J (2020) Material extrusion-based additive manufacturing of polypropylene: a review on how to improve dimensional inaccuracy and warpage. *J Appl Polym Sci*. <https://doi.org/10.1002/app.48545>
21. Adil S, Lazoglu I (2023) A review on additive manufacturing of carbon fiber-reinforced polymers: current methods, materials, mechanical properties, applications and challenges. *J Appl Polym Sci*. <https://doi.org/10.1002/app.53476>
22. Magnoni P, Rebaioli L, Fassi I et al (2017) Robotic AM system for plastic materials: tuning and on-line adjustment of process parameters. *Procedia Manuf* 11:346–354. <https://doi.org/10.1016/j.promfg.2017.07.117>
23. Walia K, Khan A, Breedon P (2021) Polymer-based additive manufacturing: process optimisation for low-cost industrial robotics manufacture. *Polymers (Basel)* 13:2809. <https://doi.org/10.3390/polym13162809>
24. Liu J, Yan J, Yu H (2021) Stress-constrained topology optimization for material extrusion polymer additive manufacturing. *J Comput Des Eng* 8:979–993. <https://doi.org/10.1093/jcde/qwab028>
25. Guo N, Leu MC (2013) Additive manufacturing: technology, applications and research needs. *Front Mech Eng* 8:215–243. <https://doi.org/10.1007/s11465-013-0248-8>
26. Wang Z, Liu R, Sparks T, Liou F (2016) Large-scale deposition system by an industrial robot (I): design of fused pellet modeling system and extrusion process analysis. *3D Print Addit Manuf* 3:39–47. <https://doi.org/10.1089/3dp.2015.0029>
27. Li L, Sun Q, Bellehumeur C, Gu P (2002) Composite modeling and analysis for fabrication of FDM prototypes with locally controlled properties. *J Manuf Process* 4:129–141. [https://doi.org/10.1016/S1526-6125\(02\)70139-4](https://doi.org/10.1016/S1526-6125(02)70139-4)
28. Rebaioli L, Magnoni P, Fassi I et al (2019) Process parameters tuning and online re-slicing for robotized additive manufacturing of big plastic objects. *Robot Comput Integr Manuf* 55:55–64. <https://doi.org/10.1016/j.rcim.2018.07.012>
29. Yaragalla S, Zahid M, Panda JK et al (2021) Comprehensive enhancement in thermomechanical performance of melt-extruded peek filaments by graphene incorporation. *Polymers (Basel)*. <https://doi.org/10.3390/polym13091425>
30. Catana D, Pop M (2021) Studies regarding simulation process to static loading of the structures obtained from polylactic acid, 3D printed. *J Appl Polym Sci*. <https://doi.org/10.1002/app.50036>
31. Felber SO, Aburaia M, Wöber W, Lackner M (2021) Parameter optimization for the 3D print of thermo-plastic pellets with an industrial robot. In: *Digital Conversion on the Way to Industry 4.0: Selected Papers from ISPR2020, September 24–26, 2020 Online-Turkey*. Springer, pp 236–247
32. İpekçi A, Ekici B (2022) Effect of fiber set-up and density on mechanical behavior of robotic 3D-printed composites. *Emerg Mater Res* 11:160–166. <https://doi.org/10.1680/jemmr.21.00120>
33. Moreno Nieto D, Casal López V, Molina SI (2018) Large-format polymeric pellet-based additive manufacturing for the naval industry. *Addit Manuf* 23:79–85. <https://doi.org/10.1016/j.addma.2018.07.012>
34. Barbosa GF, Shiki SB, Costa LC, et al (2023) Sistema de Manufatura Aditiva de Material Polimérico Robotizada e Peças Assim Obtidas. 1–41
35. Shenoy AV (1999) *Rheology of Filled Polymer Systems*. Springer, Netherlands, Dordrecht
36. Pulquerio EC, Pasotti A, Barbosa G, Shiki SB (2023) Robotic additive manufacturing system: development of mathematical modeling to prepare 3D printing processes for ABS copolymer. In: *Proceedings of the 27th International Congress of Mechanical Engineering*. ABCM

Publisher's Note Springer Nature remains neutral with regard to jurisdictional claims in published maps and institutional affiliations.

Springer Nature or its licensor (e.g. a society or other partner) holds exclusive rights to this article under a publishing agreement with the author(s) or other rightsholder(s); author self-archiving of the accepted manuscript version of this article is solely governed by the terms of such publishing agreement and applicable law.